

OPTIMIZATION OF INTERNAL FILLING OF A DRYING CHAMBER

Radivoje M. Topić¹, Nenad Lj. Čuprić², Jelena R. Topić³, Goran R. Topić⁴

¹Faculty of Mechanical Engineering, University of Belgrade, Serbia,

²Faculty of Forestry, University of Belgrade,

³ Certified designer, Energoprojekt, Belgrade, Serbia,

⁴ Certified designer, Serbiagas, Belgrade, Serbia

ABSTRACT

In this paper the influence of internal flight characteristics (mounting angle, α), dimensions (chord length and flight angle, C) and material characteristics (angle of natural sedimentation, θ , friction angle, φ) on the amount of material fed from the internal flight and the feeding period, directly influencing heat transfer by convection from the drying agent to the drying material particles, is analyzed. A new member has been introduced into the expression for the material surface when defining the amount of material on the curved internal flight.

Keywords: Drying chamber, internal flight, natural feeding angle, flight Mounting angle.

INTRODUCTION

The very process of drying is a complex nonlinear thermodynamic process, with a complex transfer of energy and movement of particulate materials, thereby changing - its status, along the drying chamber [6]. All this makes the drying process extremely difficult to model and manage by conventional methods. Proposed the application of technology Fuzzy to operate these facilities, as well as verification of work flow management and simulation [6].

Very little research directly related to the drum dryer is carried out so far. When defining the parameters rotary dryers are mostly used empirically derived relationships [6]. Analysis of management and impact parameters of the process regime and the drying chamber is shown in the literature [2]. A detailed review of research in the field of high temperature drying gave [2], and studies the process of moving material during the drying process [9] and Lisboa et al [11]. High temperature drying and pneumatic drum-like dryers are used for drying different materials, including among others shavings and sawdust [1] using part of the dried material (about 35%) as an energy source.

In pneumatic drum-like dryers the drying process consists of a marking period (relative resting) and a material feeding period from the internal flights of the drying chamber, consisting of internal flights distributed along the chamber cross-section. From the viewpoint of optimization of the internal drying chamber construction, efficient dryer operation can be achieved when the amount of material fed from the internal flights is increased and conditions for treating the largest number of particles falling from the flights with a drying agent are set.

1. MATERIALS AND METHODS

Defining an expression for the amount of material on the internal flight of the Drying chamber

From the viewpoint of the amount of material, if it is significantly higher than the amount the flights can take up then the dryer operation is not rational [3], fig. 1. In this case the external surface of the material at the bottom of the chamber is only insignificantly increased. It is used for establishing contact with the drying agent and represents part of the surface irradiated by the energy from the heated bare chamber surfaces. However, at the same time the particle surface treated by the drying agent in the process of convective heat transport as the most influential method for heat transport in the drying process is reduced on account of the reduced falling height, Fig. 1.

1.1. Expression for the amount of material on the internal flight

The area of the material cross-section (indirect material amount) on the flights is defined as:

$$S_m = S_t + S_{s1} = C \cdot R^2 \cdot \sin \frac{\Delta\beta}{2} \cdot \cos \left(\frac{\Delta\beta}{2} + \alpha \right) + \frac{R^2}{2} \cdot \left(\frac{\pi \cdot \Delta\beta}{180} - \sin \beta \right) \quad (1)$$

and represents a summation of areas of triangle S_T and segment 1, S_{S1} , Fig. 2 (it is a flat flight). According to recommendations [4] values of the non-dimensional flight parameter C , in expression (1) representing the ratio between the flight chord and the chamber radius, $C = B_l/R$ are in the range 0.2 to 0.4.

In the case of a curved flight, Fig. 2, the expression gains a new member that takes into account the area of segment 2, S_{S2} , so expression (1) becomes [8]:

FIGURE 1. Cross-section of the drying chamber showing distribution and feeding of the material

$$S_m = S_t + S_{s1} + S_{s2} = C \cdot R^2 \cdot \sin \frac{\Delta\beta}{2} \cdot \cos \left(\frac{\Delta\beta}{2} + \alpha \right) + \frac{R^2}{2} \cdot \left(\frac{\pi \cdot \Delta\beta}{180} - \sin \beta \right) + \frac{C^2 \cdot R^2}{8 \cdot \cos^2 (90 - \alpha)} \left(\frac{\pi \cdot 2\alpha}{180} - \sin 2\alpha \right) \quad (2)$$

The third member on the right represents the area of segment 2, S_{S2} , Fig. 2.

As seen in expressions (1) and (2) the material area on flights is variable and

a)

b)

FIGURE 2. Scheme for determining the area of the material on the flight (a – of a flat flight; b – of a curved flight)

is defined using the following function: $S_m = f(C, R, \Delta\beta, \alpha)$.

1.2. Expression for the angle $\Delta\beta$

The angle between the flight root and material peak on the flight along the drying chamber wall is defined as:

$$\Delta\beta = \theta - \beta + \arcsin \{ \sqrt{C^2 - 2 \cdot C \cdot \cos \alpha + 1} \cdot \sin [\beta + \Delta\beta_1] - \theta \} \quad (3)$$

Having in mind, fig.2, that the angle $\Delta\beta_1$ is defined as:

$$\operatorname{tg} \Delta \beta_1 = \frac{B_1 \cdot \sin \alpha}{R - B_1 \cdot \cos \alpha} = \frac{C \cdot R \cdot \sin \alpha}{R - C \cdot R \cdot \cos \alpha} = \frac{C \cdot \sin \alpha}{1 - C \cdot \cos \alpha} \quad (4)$$

expression (3) becomes:

$$\Delta \beta = \theta - \beta + \arcsin \left\{ \sqrt{C^2 - 2 \cdot C \cdot \cos \alpha + 1} \cdot \sin \left[\beta + \operatorname{arctg} \frac{C \cdot \sin \alpha}{1 - C \cdot \cos \alpha} \right] - \theta \right\} \quad (5)$$

or

$$\Delta \beta = \theta - \beta + \arcsin \left\{ \sqrt{C^2 - 2 \cdot C \cdot \cos \alpha + 1} \cdot \sin \left[\beta + \arcsin \frac{C \cdot \sin \alpha}{\sqrt{C^2 - 2 \cdot C \cdot \cos \alpha + 1}} \right] - \theta \right\} \quad (6)$$

The angle $\Delta \beta$ is a function of several variables: $\Delta \beta = f(\theta, \alpha, \beta, C)$.

2. RESULTS AND DISCUSSION

Analysis of the influence of material characteristics and flight dimensions on the amount of material on the flight

In order to perform this analysis, 3D diagrams of the dependence $S_m = f(C, R, \Delta \beta, \alpha)$, Fig. 3 and Fig. 4 were constructed, showing the influence of the flight mounting angle α and flight dimensions C on the value of the material area on the curved internal flight.

FIGURE 3. Dependence of the material surface on the flight mounting angle

Using the diagram given in Fig. 3 one can note that increase in the angle leads to a decrease in the material area and change in the dependence character of curve S_m . Changes in the angle values from 0 to 60°, lead to reduction of surface S_m for about 59%. The same diagram can be used to evaluate that the material type (Fig. 4., using angle θ) significantly influences changes in the value of S_m . For materials whose natural feeding angle is 60° the most favorable flight mounting angle is 0°. However, this is not good from the viewpoint of the feeding period.

To define the moment when the blade is empty, Fig.5. Pouring end of the period, it is important to define the mobility coefficient of the material:

FIGURE 4. Angle of natural repose

FIGURE 5. The moment when the blade is Empty,

$$I = \frac{\tau_{\text{pouring}}}{\tau_{\text{aging}}} \quad (7)$$

FIGURE 6. Dependence of the material area on the flight dimensions

The diagram given in Fig.6 shows a linear dependence of the material area S_m on the value of the ratio between the flight chord and the drying chamber radius, C . Increasing this ratio for 100%, i.e. flight width when the mounting angle is α leads to an increase in S_m area of about 32%. This increase is larger for materials with a higher natural feeding angle. Diagrams given in Fig. 7, Fig. 8 and Fig. 9, are 3D diagrams of the dependence $\Delta \beta = f(\theta, \alpha, \beta, C)$ showing the influence of the flight mounting angle α and position

β , dimensions of the drying chamber or flight, C and characteristics of the material through the angle θ , on values of angle $\Delta\beta$, i.e. material area on the flight, S_m .

FIGURE 7. Dependence of the angle $\Delta\beta$ on the flight position angle and mount position

FIGURE 8. Dependence of the angle $\Delta\beta$ on the flight position angle and material characteristics

For curved flights the null value of angle $\Delta\beta$ does not mean a null value of the material on the flight.

The presented analysis enables determination of a negative value of angle $\Delta\beta$ for which the curved flight is completely empty.

FIGURE 9. Dependence of angle $\Delta\beta$ on flight dimensions

3. CONCLUSION

From the viewpoint of optimization of the construction of the internal filling of the drying chamber one should select such dimensions, flight shapes and conditions that enable falling of optimal amounts of material from the flights during the drying process, thus increasing the material feeding time and enabling treatment of the largest number of particles with a drying agent.

A new member was introduced by the author in the analytical expression for the area or volume of the material when analyzing the amount of material on a curved flight.

The presented diagrams enable determination of the material area on the flight, S_m , for a set value of the mounting angle α , flight parameter C and flight position angle β .

Analysis of the influence of characteristic parameters of the material and flights on the material area values is also possible.

Dependence of the material area on the flight on angle $\Delta\beta$ enables determination of the moment when the flight (straight or curved) becomes completely empty after feeding the material.

Changes of angle $\Delta\beta$ enable analysis of changes in the material amount on the flight during the feeding period from the viewpoint of the material type, flight position, flight mounting angle, dimensions of the drying chamber or internal flights.

NOMENCLATURE

- B flight width, chord length m;
- C ratio between the flight chord and drying chamber radius;
- F material area on flights m^2 ;
- h material feeding height m;
- n number of rotations of the drying chamber s^{-1} ;
- R drying chamber radius m;
- S material area on one flight m^2 ;

Greek letters

- α Flight mounting angle,
 β Flight position angle,
 θ Angle of natural sedimentation;
 γ Angle between the chord and material area on the flight;
 φ Angle of friction between the material and the flight and drying chamber surface

Subscripts

- L flight
m material
s segment

ACKNOWLEDGEMENTS

Project NPEE 263004 Ministries for Science and Environment Protection of the Republic of Serbia, National Energy Efficiency Program (2006).

REFERENCES

1. Topic, M. R. (2006). Project NPEE 263004, Ministry of Science and Environment of the Republic of Serbia National Energy Program efficiency.
2. Topic, M. R. (1996). Analysis, optimization and modeling of processes and solutions high temperature drying, Monograph, Faculty of Mechanical Engineering, Belgrade.
3. Valušis, V. J. (1977). Fundamentals of high temperature in shavings materials, "Kolos", Moscow.
4. Severnjov, M. M.; Terpilovskij, I. F.; Majonov, V. V. (1980). Mechanical separation of moisture and thermal drying of wet materials, "Kolos" Moscow.
5. Topić, M. R.; Vasiljević, M. B. (1996). Modeling and optimization of the pneumatic Rotary high temperature dryer inner structure, Proceedings of the 10 th International Drying Symposium, Volume A, Krakow, Poland.
6. Kemp, I.C. (2004). Comparison of Particle Motion Correlations for Cascading Rotary Dryers, Proceedings of the 14th International Drying Symposium (IDS 2004), Vol. B, Sao Paulo (790-797).
7. Pirrello, L.; Yliniemi, L.; Leiviska, K.; Galluzzo M. (2002). Self-tuning fuzzy control of a rotary dryer, Proc. of The Triennial World Congress, IFAC, Barcelona.
8. Topić, M.R. (2008). Optimization of internal filling of a drying chamber of a high temperature pneumatic drum - like dryer from the viewpoint of the amount of material, Proceedings of the 16th International Drying Symposium, Mumbai (702-705).
9. Britton, P. F.; Sheehan, M.E.; Schneider P.A. (2006). A Physical Description of Solids Transport in Flighted Rotary Dryers, Powder Technology № 165 (153-160).
10. Lee, A.; Sheehan, M. E. (2010). Development of a Geometric Flight Unloading Model

for lighted Rotary Dryers, Powder Technology № 198 (395-403).

11. Lisboa, M.H.; Vitorino, D.S.; Delaiba, W.B.; Finzer J.R.D.; Barrozo M.A.S. (2004). A Study of Particle Motion in Rotary Dryer, Brazilian Journal of Chemical Engineering, № 03, Vol. 24 (365-374):

Figure and Tables

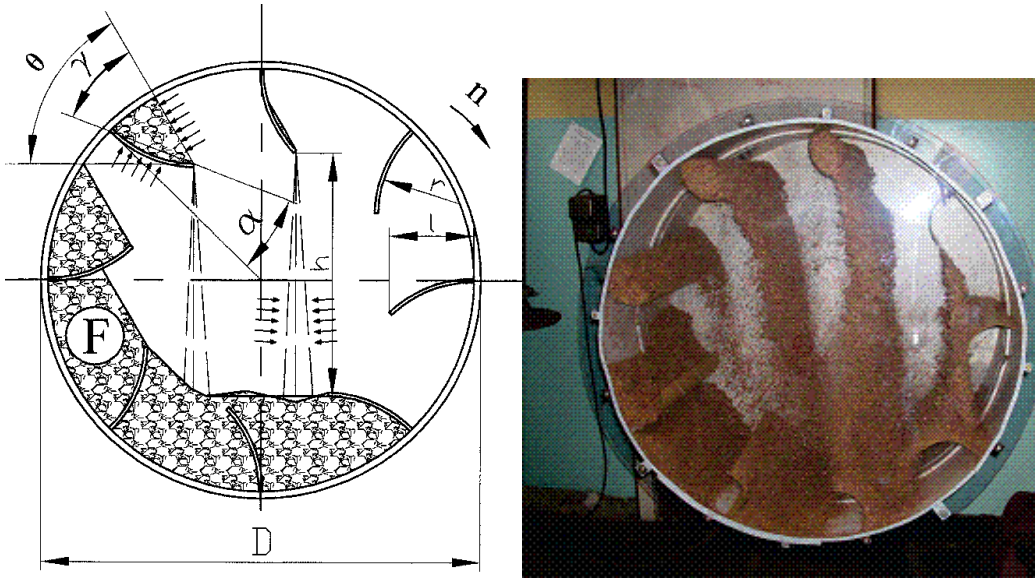


FIGURE 1. Cross-section of the drying chamber showing distribution and feeding of the material

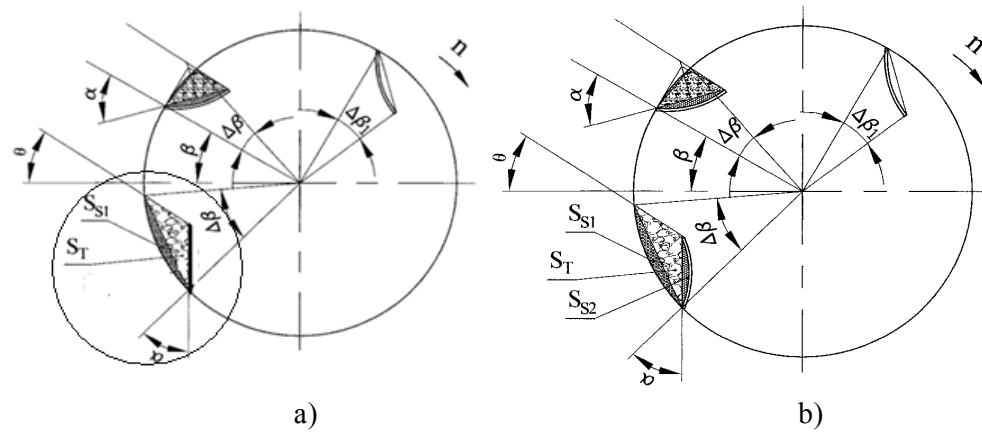


FIGURE 2. Scheme for determining the area of the material on the flight (a – of a flat flight; b – of a curved flight)

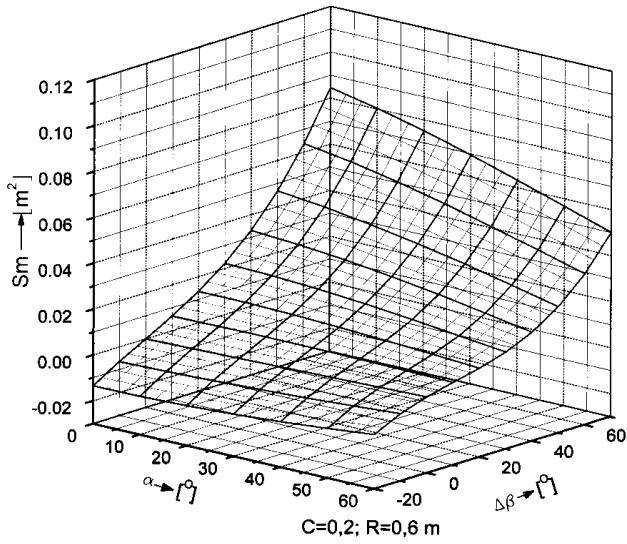


FIGURE 3. Dependence of the material surface on the flight mounting angle

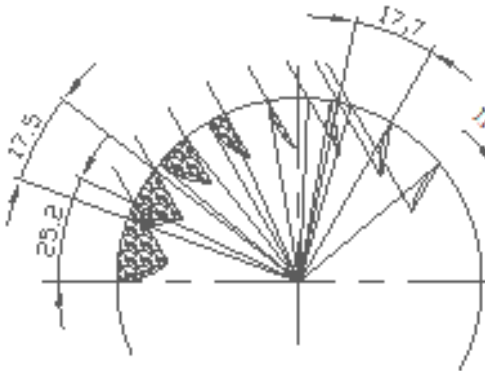
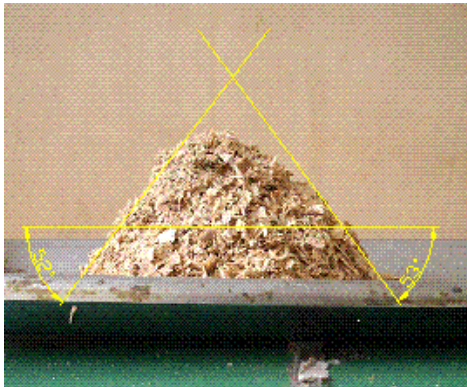


FIGURE 4. Angle of natural repose

FIGURE 5. The moment when the blade is

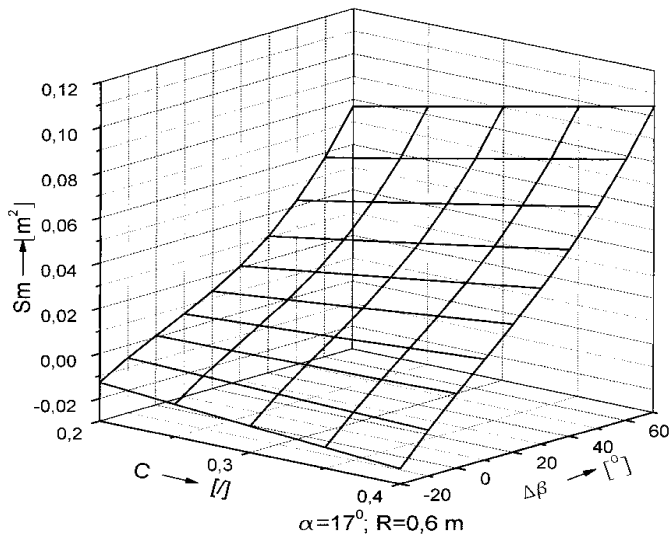


FIGURE 6. Dependence of the material area on the flight dimensions

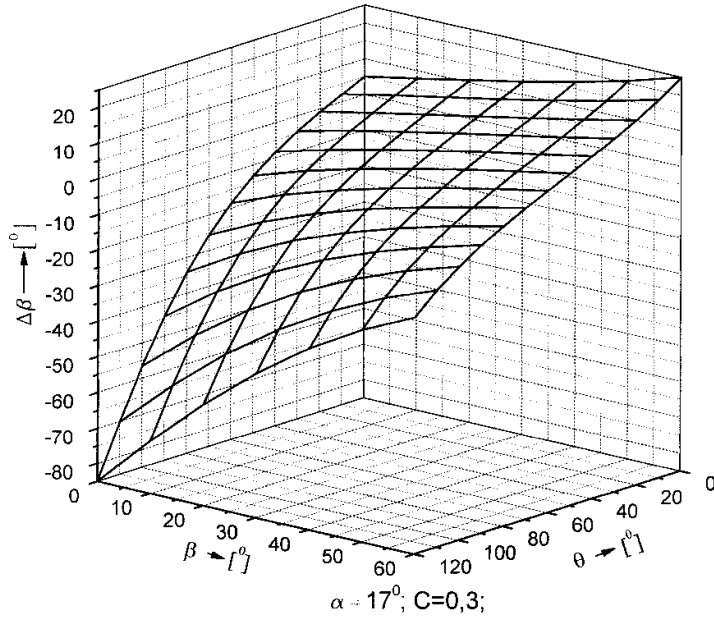


FIGURE 7. Dependence of the angle $\Delta\beta$ on the flight position angle and mount

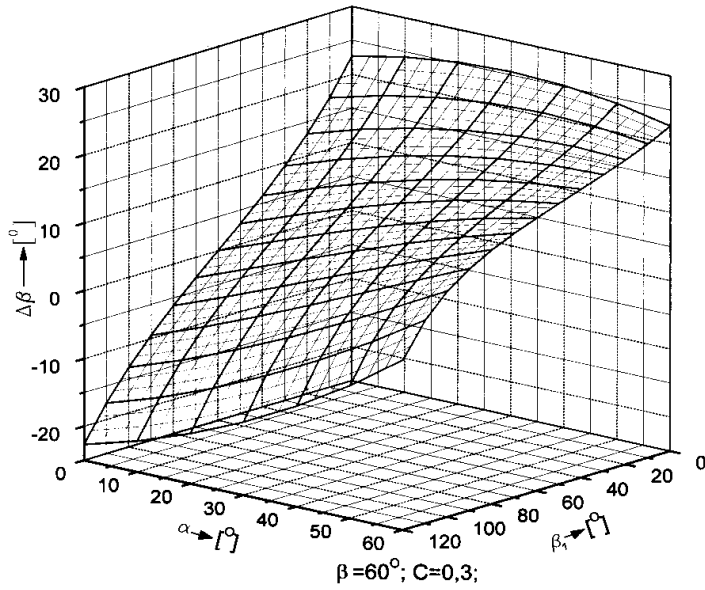


FIGURE 8. Dependence of the angle $\Delta\beta$ on the flight position angle and material characteristics

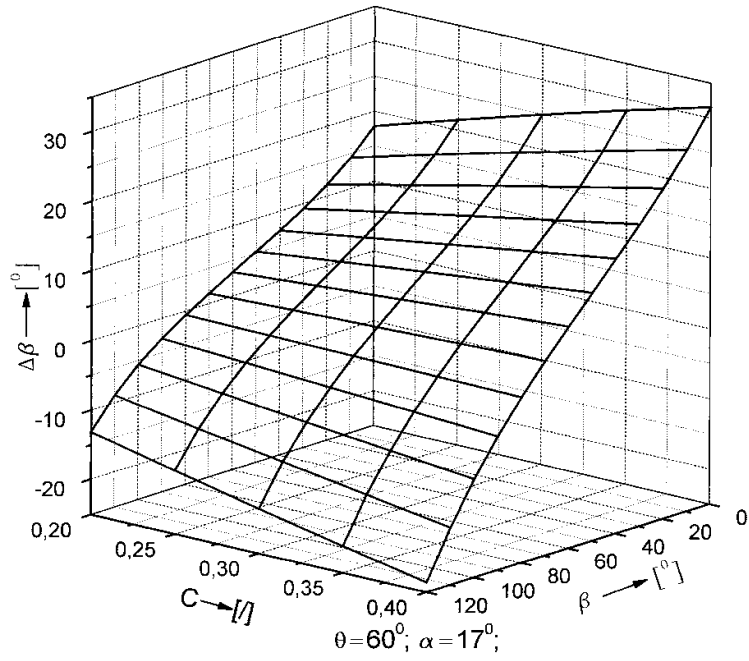


FIGURE 9. Dependence of angle $\Delta\beta$ on flight dimensions